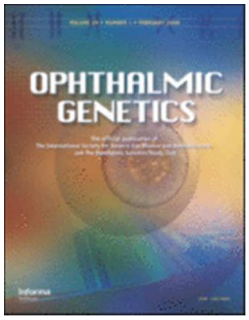

CNGB3 Mutations Cause Severe Rod Dysfunction.

Journal:	*Ophthalmic Genetics*
Manuscript ID	NOPG-2017-0027.R2
Manuscript Type:	Case Report
Date Submitted by the Author:	n/a
Complete List of Authors:	Maguire, John; University of Bradford, School of Optometry & Vision Sciences McKibbin, Martin; St. James's University Teaching Hospital, Department of Ophthalmology Khan, Kamron; St. James's University Teaching Hospital, Department of Ophthalmology Kohl, Susanne; Ophthalmic Research, Molecular Genetics Ali, Manir; University of Leeds, Leeds Institute of Biomedical and Clinical Sciences McKeefry, Declan; University of Bradford, School of Optometry & Vision Sciences
Keywords:	achromatopsia, rods, electroretinogram

CNGB3 Mutations Cause Severe Rod Dysfunction.

J. Maguire[1], M. McKibbin[2], K. Khan[2], Susanne Kohl[3], Manir Ali[4] & D. McKeefry[1]

[1]School of Optometry and Vision Sciences, Bradford University, UK.

[2]Department of Ophthalmology, St. James's University Teaching Hospital, Leeds, UK

[3] Molecular Genetics Laboratory, Institute of Ophthalmic Research, Centre of Ophthalmology, University Clinics Tubingen, Tubingen, Germany

[4] Section of Ophthalmology and Neuroscience, Leeds Institute of Biomedical and Clinical Sciences, University of Leeds, Leeds, UK

Corresponding Author: Declan McKeefry
School of Optometry and Vision Science, University of Bradford, Bradford, West Yorkshire, BD7 1DP, UK
Email: d.mckeefry@bradford.ac.uk
Tel: +44(0)1274 234648.

Abstract

Purpose: Congenital achromatopsia or rod monochromatism is a rare autosomal recessive condition defined by a severe loss of cone photoreceptor function in which rods purportedly retain normal or near-to-normal function. This report describes the results of electroretinography in two siblings with *CNGB3*-associated achromatopsia.

Methods: Full field light- and dark-adapted ERGs were recorded using standard protocols detailed by the International Society for Clinical Electrophysiology of Vision (ISCEV). We also examined rod mediated ERGs using series of stimuli that varied over a 6 log unit range of retinal illuminances (-1.9 – 3.5 log scotopic Trolands).

Results: Dark-adapted ERGs in achromatopsia patients exhibited severely reduced b-wave amplitudes with abnormal b:a ratios (1.3 and 0.6). In comparison, the reduction in a-wave amplitude was less marked. The rod mediated ERG took on an electronegative appearance at high stimulus illuminances.

Conclusion: Although the defect that causes achromatopsia is primarily in the cone photoreceptors, our results reveal an accompanying disruption of rod function that is more severe than has previously been reported. The differential effects on the b-wave relative to the a-wave, points to an inner-retinal locus for the disruption of rod function in these patients.

Key words: achromatopsia, rods, electroretinogram

Introduction

Complete achromatopsia (ACHM), also known as rod monochromacy, is a rare autosomal recessive congenital condition with a prevalence of 1:30,000, characterised by complete or partial loss of cone function [1]. Clinically, patients present with photophobia, nystagmus, severely reduced visual acuity (20/200) and severe colour vision deficits [2]. Currently, six genes have been implicated in the generation of this disease, all of which encode crucial steps in the cone photo-transduction cycle. Two genes encoding for the cyclic nucleotide gated (CNG) channels alpha (α) and beta (β) (CNGA3, CNGB3) account for approximately 25% and 60% of the all mutations, respectively, with the rarer mutations found in the *GNAT2*, *PDE6C*, *PDE6H*, *ATF6* genes [1, 3]. Over 140 mutations have been discovered in the *CNGA3* and *CNGB3* genes, most of which result in a failure to produce α or β subunits. In the normal functioning retina the CNG channels, located in the plasma membrane of the outer segment, are held open in darkness by cyclic guanosine monophosphate (cGMP), creating an inward positive current. When light causes hydrolysis of cGMP the channels are closed causing a hyperpolarisation of the cell; without functional subunits, CNG channels remain constantly closed, preventing cone hyperpolarisation. In adults this can frequently result in the degeneration of cone photoreceptors. However, evidence of foveal disruption and hypoplasia has also been shown in young children [4 -7]. In a few cases, some residual cones may remain, although they too may later progressively decline [7-9].

In the light of the above findings, the canonical view of congenital ACHM has been that it is a condition that primarily leads to cone dysfunction, leaving rod photoreceptoral function largely intact [1,2,10-17]. However, the phenotype is highly variable and a growing body of experimental evidence indicates that ACHM may not only lead to structural and functional abnormalities within the cone photoreceptor population, but also may affect rod function as well. Rod dysfunction in ACHM, as assessed using ERG, has been noted in several studies, typically ranging from a mild [6, 18-22] to a moderate reduction in the rod ERG amplitude

[23-25]. This can make discrimination between achromatopsia and cone-rod dystrophy (CORD) more difficult. Previously, the understanding was that the former was typically a stationary disease, associated with a normal rod ERG, whereas the latter was progressive in nature, affecting both rods and cones [26]. An additional confounding factor is that both CNGA3 and CNGB3 genes have been implicated in autosomal recessive cone rod dystrophy (arCORD) [23-28]. In addition, structural changes more frequently associated with CORD, such as macular atrophy, have been reported in achromatopsia [14, 22]. In essence, the changes in amplitude noted to the rod ERG in achromatopsia generally remain in the sub-normal to moderate category compared to severely reduced or abolished rod response found in CORD [12, 25].

In this report we present electro-retinographic results from two siblings with a homozygous 1148delC (Thr383fs) mutation in CNGB3. Interestingly, both of these siblings exhibit ERG findings which show severe disruption of the rod system, specifically confined to the inner retina, resulting in an electronegative ERG.

Materials and Methods

Participants and clinical assessment

Two siblings from a consanguineous Pakistani family living in the UK, both with molecularly confirmed *CNGB3*-associated ACHM were examined (see table 1 for a summary of the main features). In brief, the patients were first examined at 1 year of age presenting with the classical features of ACHM - congenital nystagmus, reduced vision and photophobia. Over three decades changes in visual function have been minimal, with VA having remained constant. The most significant changes have been structural with progressive macular atrophy being noted on successive retinal examinations. The patients do not report any symptoms of nyctalopia and prefer conditions of low illumination.

At the time of this study the patients were 31 yrs (Px1) and 38 yrs (Px 2) old and full clinical history and assessment of the participants was performed which included Snellen visual acuity, colour vision testing using the Colour Assessment and Diagnosis (CAD) Test (City University, London), as well as Ocular Coherence Tomography (OCT). In addition, Goldmann visual fields (Haag Streit, Bern, Switzerland) were assessed using the largest target on both ACHM patients (see figure 1). The subjects gave informed consent prior to the commencement of the experiments and the study was conducted using a process that had been approved by the Leeds Research Ethics Committee and met the tenets of the Helsinki declaration.

Table 1 and figure 1 here

Genetic Assessment

One of the siblings (Patient 1) had previously been recruited to an earlier study investigating the molecular genetic basis for inherited retinal disease (IRD). As part of this study, patients' DNA was analysed by Sanger sequencing of genes known at that time to be associated with ACHM in a step-by-step procedure. The proband was found to be homozygous for a null allele in *CNGB3* (NM_019098.4; c.1148delC, p.T383Ifs*13), the most frequently reported cause of ACHM in those of European ancestry [29]. Segregation analysis confirmed that Patient 2 was also homozygous for the c.1148delC allele.

Electrophysiological Assessment

Full-field ERGs were recorded using a ColorDome (Diagnosys LLC, Lowell, MA, USA) four primary ganzfeld stimulator and were obtained using standard protocols detailed by the International Society for Clinical Electrophysiology of Vision (ISCEV) [30]. The light-adapted (LA) single flash and 30Hz flicker stimuli (both 3.0 cd/s/m^2) were used to assess the cone system. Following a period of 20 minutes dark adaptation, a 0.01cd/s/m^2 (DA0.01) and 10.0 cd/s/m^2 (DA10.0) flash stimuli were used to elicit rod responses. In addition to the standard ISCEV stimuli we also examined rod mediated ERGs in our patient group and an age-matched control using series of stimuli that varied over a wider range (~ 6 log units) of retinal illuminance from -1.9 – 3.6 log scotopic trolands. ERGs were recorded using these stimuli which consisted of brief (4ms) white flashes delivered after 20 mins of dark adaptation.

ERGs were recorded from the right eye using a silver/nylon corneal fibre electrode (Dept. of Physics and Clinical Engineering, Royal Liverpool University Hospital, UK) referenced to a 9mm Ag/AgCl electrode (Biosense Medical, Chelmsford, UK) on the outer canthus; a similar electrode was placed on the forehead to serve as ground. Impedance was maintained below

5 kΩ. Signals were recorded using the Espion E^2 system (Diagnosys LLC, Lowell, MA, USA) which amplified and filtered (bandwidth = 1 to 300 Hz) the ERGs and digitised them at a rate of 1000Hz. Participants viewed the stimuli monocularly with a dilated pupil (1% Tropicamide).

Figure 2 and Table 2 here

Results

Figure 2 shows the standard ISCEV full-field ERG responses from the ACHM patients as well as a set of responses from a representative age-matched normal subject. The light-adapted single flash and the photopic flicker responses were undetectable in both ACHM patients, consistent with the severe cone dysfunction typically reported for this condition [23]. The DA0.01 responses were also abnormal, with a severe loss of b-wave amplitude (Table 2). Patient 1's responses are reduced by 74%, whilst Patient 2 has lost 87% of their b-wave amplitude compared to our normal mean value. The DA10.0 waveforms also exhibit significant loss of b-wave amplitude, and for Patient 2 the waveforms are electronegative. A smaller reduction is noted in a-wave amplitude which may be explained by the loss of input from the dark adapted cone system [31]. Implicit times of the a- and b-waves are also increased compared to normative data (see table 2).

Figure 3 here

Figure 3 shows the ERG waveforms for dark adapted ERGs recorded as a function of retinal illuminance across a 6 log unit scale (-1.9 – 3.6 log scot trolands). The data show clear

qualitative differences between the ERG waveforms obtained from an individual with normal rod function compared to those obtained from the 2 rod monochromats across the same illuminance range. In particular, the responses generated at low retinal illuminances (-1.9 – -0.9 log scot trolands) are markedly attenuated in the rod monochromats compared to the normal ERGs. In fact b-wave amplitude is reduced across the whole illuminance range in the rod monochromats and again the development of the electronegative response in Patient 2 can be clearly observed beyond 1.1 log scot trolands.

Figure 4 here

In Figure 4 peak amplitudes and implicit times of the a- and b-waves have been plotted as a function of retinal illuminance for a normal control participant and the ACHM patients 1 and 2. As indicated by the waveforms in Figure 3, the greatest difference is in b-wave amplitude (fig 4A). The illuminance response function from the normal subject exhibits an initial steep increase in b-wave amplitude up to 1 log scot troland after which it reaches saturation. This saturating response function of the dark adapted ERG has been described previously and is considered to be the result of an algebraic interaction between receptoral and post-receptoral retinal responses at higher illuminances [32, 33]. In contrast, the b-wave amplitude illuminance-response functions from the two monochromats are markedly different; with b-wave amplitude exhibiting a much shallower, monotonic increase with increasing retinal illuminance. The illuminance response of the a-wave (fig 4C), by comparison, appears to be similar across the rod monochromats and the normal. In terms of a- and b-wave implicit times (fig 4B & D) the biggest differences between the control subject and patients occur at low retinal illuminances (< 1 log scot trolands) where the ERGs from the rod monochromats have considerably longer a- and b-wave implicit times. However, as

retinal illuminance increases the differences in implicit times between the normal and the achromatopsic patients becomes less marked.

Discussion

In this case study we have reported the results of visual electrophysiology in two siblings with *CNGB3*-associated achromatopsia and have demonstrated the existence of an unusually severe deficit of rod-mediated retinal function. As would commonly be expected in cases of complete ACHM, electroretinography reveals a complete loss of cone function. However, this deficit is also accompanied by marked abnormalities of the rod mediated dark-adapted b-wave ERG responses. Whilst *CNGB3* mutations with moderate rod dysfunction have previously been reported in the literature [21-24] we are not aware of any cases demonstrating such severe rod involvement as exhibited by the individuals examined here. In particular, the electronegative appearance of the dark-adapted ERGs to more intense stimuli is a previously unreported finding for this specific mutation.

Rod function was assessed using standard ISCEV protocols. The dark-adapted (DA) rod stimulus (0.01 cd/s/m^2) elicits an ERG in the normal population that is typically dominated by a large positive component (the b-wave) with a peak occurring at approximately 100 ms after stimulus onset. This response reflects the activity of rod ON-bipolar cells from the inner nuclear layer of the retina [34, 35]. As the intensity of the stimulus is increased, the b-wave is preceded by a negative a-wave in the dark-adapted ERG, which predominantly reflects activity in the outer segments of the rod photoreceptors [31, 35]. The data presented here show that patients with *CNGB3* associated achromatopsia have significant functional abnormalities in their rod system which accompanies severe cone dysfunction. This rod dysfunction is in the ACHM patients is manifest in the severely attenuated b-wave amplitudes of the dark adapted ERGs. In comparison, the a-waves of these responses are

less drastically affected. Whilst there is some reduction in a-wave amplitude across the illuminance range tested (something which most likely attributable to the loss of contribution from the dark adapted cones [31, 35]), on the whole, a-wave amplitudes in the ACHM patients are comparable to normals. This differential effect on the b- and a-waves has not previously been reported and is significant because it points to a post-receptoral, inner retinal origin for this loss of rod function. It suggests that the deficit is at the level of the rod ON-bipolar cells, rather than at the level of the rod photoreceptors.

The reasons for the deficits in rod-mediated retinal function are not entirely clear. It is unlikely to be simply an age-related loss of rod function. The ages of the two ACHM patients in this study fall well within the range of previous study [5] where the ACHM patient cohort exhibits milder rod deficits than those reported here. Furthermore, the study by Moskowitz and colleagues [24] report rod deficits in a much younger group (median age 2.7 yrs) of ACHM patients. Genetic testing for the patients examined in this study was performed by successive Sanger sequencing of the following genes until a cause was identified (CNGA3, CNGB3, GNAT2, PDE6C). There remains the slim possibility that the family also segregate another monogenic retinopathy. However, the fact that the ERG shows a near normal a-wave with more severe b-wave reduction, specifically suggests a predominantly inner retina dysfunction, which is not a classical feature associated with cone-rod dystrophy. A more likely explanation is that the environment created by degenerating cones may play a part in the generation of dysfunction in rod-mediated vision. Macular atrophy was an acquired feature in both patients suggesting there is some outer retinal degeneration at the macula and supporting the idea that rod dysfunction may be a secondary feature of cone death. In addition, work in mouse models has shown significant correlations between cone cell death and CNG channel abnormalities. A recent review of cone cell death in achromatopsia [36] has outlined several mechanisms that may contribute to cone apoptosis; stress markers associated with the endoplasmic reticulum are increased in CNGA3$^{-/-}$ and CNGA3$^{-/-}$ knockout

mice. Abnormal levels of cellular $Ca2^{++}$ or cGMP often associated with ACHM have been shown to increase endoplasmic reticulum stress [37].

Recent advances in adaptive optics have made it possible to examine the structure of the both inner and outer segments of the photoreceptor layer in vivo using adaptive optics scanning laser ophthalmoscopy (AOSLO) [38, 39]. Imaging in patients with ACHM has shown significant loss and disruption of cone photoreceptors, but no real evidence of a decrease in the number of rods [5, 7]. However, changes in rod structure have been observed. Typically, the diameter of a rod photoreceptor in a healthy retina at 10^{o} eccentricity is approximately 2.3μm. Measurements of rod diameter in patients with ACHM in a similar region were shown to be on average 1μm greater [4]. This increase in diameter may be as a direct result of increased space in the retina which allows rods to expand following the loss of cone cells [24]. Increases in rod diameter naturally occur in the ageing retina as the overall number of rod cells is reduced [40]. It has been suggested that structural changes like these may well result in an alteration of the photo-transduction process and even post-receptoral connections [24].

In summary, we believe this report further adds to the evidence that achromatopsia associated with a homozygous mutation in the CNGB3 gene can lead to abnormalities of rod mediated vision as well cone dysfunction. More significantly, we have shown for the first time, the presence of an electronegative ERG that occurs as a consequence of this mutation. The deficits in the rod responses reported here are more severe than those that have been previously reported in ACHM patients. A key finding of this study is that it is the rod b-wave that is more severely affected, compared to the a-wave, which is relatively well preserved. This points to a post-receptoral/inner retinal site for the pathological changes in rod function found in these patients.

References

[1] Remmer MH, Rastogi N, Ranka MP, Ceisler, EJ. Achromatopsia: a review. *Curr Opin Ophthalmol.* 2015; 26(5): 333-340.

[2] Eksandh L, Kohl S, Wissinger B. Clinical features of achromatopsia in Swedish patients with defined genotypes. *Ophthal Genet.* 2002; 23(2):109-120.

[3] Kohl S, Zobor D, Chiang W-C et al. Mutations in the unfolded protein response regulator ATF6 cause the cone dysfunction disorder achromatopsia. *Nat Genet.* 2015;47(7):757-765.

[4] Carroll J, Choi SS, Williams DR. In vivo imaging of the photoreceptor mosaic of a rod monochromat. *Vis Res.* 2008; 48(26):2564-2568.

[5] Genead MA, Fishman GA, Rha J et al. Photoreceptor structure and function in patients with congenital achromatopsia. *Invest Ophthalmol Vis Sci*. 2011; 52(10):7298-7308.

[6] Yang P, Michaels KV, Courtney RJ et al. (2014) Retinal morphology of patients with achromatopsia during early childhood: implications for gene therapy. *JAMA Ophthalmology* 2014; 132:823-31.

[7] Langlo CS, Patterson EJ, Higgins BP et al. Residual Foveal Cone Structure in CNGB3-Associated Achromatopsia. *Invest Ophthalmol Vis Sci*. 2016; 57(10):3984-3995.

[8] Thiadens AA, Somervuo V, van den Born LI et al. Progressive loss of cones in achromatopsia: an imaging study using spectral-domain optical coherence tomography. *Invest Ophthalmol Vis Sci*. 2010; 51(11): 5952-5957.

[9] Thomas MG, McLean RJ, Kohl S et al. Early signs of longitudinal progressive cone photoreceptor degeneration in achromatopsia. *Brit J Ophthalmol.* 2012; 96:1232-1236.

[10] Kohl S, Hamel CP. Clinical utility gene card for: achromatopsia. *Eur J Hum Genet.* 2011: 19(6): doi:10.1038/ejhg.2010.231.

[11] Ouechtati F, Merdassi A, Bouyacoub Y et al. Clinical and genetic investigation of a large Tunisian family with complete achromatopsia: identification of a new nonsense mutation in GNAT2 gene. *J Hum Genet.* 2011; 56:22-8.

[12] Saqib MA, Awan BM, Sarfraz M et al. (2011) Genetic analysis of four Pakistani families with achromatopsia and a novel S4 motif mutation of CNGA3. *Jap J Ophthalmol*. 2011; 55:676-80.

[13] Wawrocka A, Kohl S, Baumann B et al. Five novel CNGB3 gene mutations in Polish patients with achromatopsia. *Molecular Vis.* 2014; 20:1732-9.

[14] Katagiri S, Hayashi T, Yoshitake K et al. Congenital Achromatopsia and Macular Atrophy caused by a Novel Recessive PDE6C Mutation (p.E591K). *Ophthalmic Genet.* 2015; 36:137-44.

[15] Liang X, Dong F, Li H et al. Novel CNGA3 mutations in Chinese patients with achromatopsia. *Brit J Ophthalmol.* 2015; 99:571-6.

[16] Kuniyoshi K, Muraki-Oda S, Ueyama H et al. (2016) Novel mutations in the gene for alpha-subunit of retinal cone cyclic nucleotide-gated channels in a Japanese patient with congenital achromatopsia. *Jap J Ophthalmol.* 2016; 60:187-97.

[17] Ueno S, Nakanishi A, Kominami T et al. In vivo imaging of a cone mosaic in a patient with achromatopsia associated with a GNAT2 variant. *Jap J Ophthalmol.* 2017; 61:92-98.

[18] Eksandh L, Kohl S, and Wissinger, B. Clinical features of achromatopsia in Swedish patients with defined genotypes. *Ophthalmic Genet.* 2002; 23:109-20.

[19] Doucette L, Green J, Black C et al. Molecular genetics of achromatopsia in Newfoundland reveal genetic heterogeneity, founder effects and the first cases of Jalili syndrome in North America. *Ophthalmic Genet.* 2013; 34:119-29.

[20] Kurent A, Stirn-Kranjc B. and Brecelj, J. Electroretinographic characteristics in children with infantile nystagmus syndrome and early-onset retinal dystrophies. *Eur J Ophthalmol.* 2015; 25:33-42.

[21] Nishiguchi KM, Sandberg MA, Gorji N et al. Cone cGMP-gated channel mutations and clinical findings in patients with achromatopsia, macular degeneration, and other hereditary cone diseases. *Hum Mutat.* 2005; 25:248–258.

[22] Sundin OH, Yang JM, Li Y et al. Genetic basis of total colour blindness among the Pingelapese islanders. *Nat Genet.* 2000; 25:289–29.

[23] Khan NW, Wissinger B, Kohl S, Sieving PA. CNGB3 achromatopsia with progressive loss of residual cone function and impaired rod-mediated function. *Invest Ophthalmol Vis Sci*. 2007; 48:3864-71.

[24] Moskowitz A, Hansen RM, Akula JD et al. (2009) Rod and rod-driven function in achromatopsia and blue cone monochromatism. *Invest Ophthalmol Vis Sci*. 2009; 50:950-8.

[25] Li S, Huang L, Xiao X et al. (2014) Identification of CNGA3 mutations in 46 families: common cause of achromatopsia and cone-rod dystrophies in Chinese patients. *JAMA Ophthalmol.* 2014; 132:1076-83.

[26] Michaelides M, Aligianis IA, Ainsworth JR et al. Progressive cone dystrophy associated with mutation in CNGB3. *Invest Ophthalmol Vis Sci*. 2004; 45:1975-82.

[27] Thiadens AA, Roosing S, Collin RW et al. (2010) Comprehensive analysis of the achromatopsia genes CNGA3 and CNGB3 in progressive cone dystrophy. *Ophthalmol.* 2010; 117: 825-30.e1.

[28] Shaikh RS, Reuter P, Sisk RA et al. Homozygous missense variant in the human CNGA3 channel causes cone-rod dystrophy. *Eur J Hum Genet*. 2015; 23:473-80.

[29] Kohl S, Varsanyi B, Antunes GA et al. CNGB3 mutations account for 50% of all cases with autosomal recessive achromatopsia. *Eur J Hum Genet.* 2005:13(3):302-308.

[30] McCulloch DL, Marmor MF, Brigell MG et al. ISCEV Standard for full-field clinical electroretinography (2015 update). *Doc Ophthalmol.* 2015; 130(1): 1-12.

[31] Robson JG, Frishman LJ. The rod-driven a-wave of the dark-adapted mammalian electroretinogram. Prog Ret Eye Res., 2014; 39:1-22.

[32] Peachey NS, Alexander KR, Fishman GA. The luminance-response function of the dark-adapted human electroretinogram. *Vis Res.* 1989*;* 29(3):263-270.

[33] Wali N, Leguire LE. Dark-adapted luminance-response functions with skin and corneal electrodes. Doc Ophthalmol. 1989; 76(4): 367-375.

[34] Stockton RA, Slaughter MM. b-Wave of the electroretinogram: a reflection of ON bipolar cell activity. *J Gen Physiol* 1989; 93:101–22.

[35] Robson JG, Frishman LJ. Dissecting the dark-adapted electroretinogram. *Doc Ophthalmol.* 1998; 95(3-4):187-215.

[36] Carvalho, L. S. and Vandenberghe, L. H. Understanding Cone Photoreceptor Cell Death in Achromatopsia. *Retinal Degenerative Diseases.* Springer. 2016 231-236

[37] Thapa A, Morris L, Xu J et al. Endoplasmic Reticulum Stress-associated Cone Degeneration in Cyclic Nucleotide-gated Channel Deficiency. *Invest Ophthalmol Vis Sci.* 2012*;* 53(14): 4282-4282.

[38] Dubra A, Sulai Y, Norris JL et al. Noninvasive imaging of the human rod photoreceptor mosaic using a confocal adaptive optics scanning ophthalmoscope. *Biomed Opt Exp.* 2011; 2(7): 1864-1876.

[39] Scoles D, Sulai YN, Langlo CS et al. In Vivo Imaging of Human Cone Photoreceptor Inner SegmentsIn Vivo Imaging of Photoreceptor Inner Segments. *Invest Ophthalmol Vis Sci.* 2014; 55(7):4244-4251.

[40] Werner J. Night vision in the elderly: consequences for seeing through a “blue filtering” intraocular lens. *Brit J Ophthalmol.* 2005*;* 89(11):1518-1521.

Patient	Sex	Age	Symptoms	VA	Fundus
Px 1	Male	34yrs	Nystagmus Photophobia, no colour vision	CF (RE & LE)	Severe macular atrophy,
Px 2	Female	38yrs	Nystagmus, Photophobia, no colour vision	2/60 (RE & LE)	Severe macular atrophy,

Table 1. Summary of the main clinical details of the ACHM patients.

Patients	Light adapted Single Flash ERG	Light adapted Flicker ERG	Dark adapted 0.01 cd/s/m^2 ERG	Dark adapted 10.0 cd/s/m^2 ERG
Px 1				
a-wave amp	X	X	----	85.0
b-wave amp	X	X	42.16	114.37
a-wave lat	X	X	----	16.0
b-wave lat	X	X	114.0	57.0
Px 2				
a-wave amp	X	X	----	83.93
b-wave amp	X	X	21.25	44.39
a-wave lat	X	X	----	14.0
b-wave lat	X	X	90.0	57.0
Normal				
a-wave amp	17.95 ± 1.87	----	----	131.35 ± 10.92
b-wave amp	82.38 ± 7.85	47.17 ± 5.41	163.15 ± 15.88	271.01 ± 14.82
a-wave lat	15.15 ± 0.36	----	----	12.82 ± 0.53
b-wave lat	28.75 ± 0.37	26.24 ± 0.52	92.33 ± 3.02	50.66 ± 2.37

Table 2. Summary of the amplitude (amp) and latency (lat) measurements for ERGs elicited by the standard ISCEV protocols. X denotes that no data could be obtained as the waveform component was undetectable, --- denotes that no measurements were taken for that particular component. Normal values are based on n=70 subjects assessed in the University of Bradford Electrodiagnostic Unit.

Figure Legends

Figure 1. a) Goldman visual field plots, and b) fundus photographs for RE only of ACHM patients 1 & 2. c) Colour discrimination thresholds plotted on a CIE 1931 (xy) chromaticity diagram for 16 different coloured targets along red, green, blue & yellow colour axes. Normal colour discrimination thresholds (+/- 1 SD) are indicated by the central grey ellipse. Both rod monochromats (only data from Patient 2 are shown) exhibit elevated discrimination thresholds consistent with severe L-, M- and S-cone dysfunction. d) OCT image of macular region of the RE of ACHM patient 1.

Figure 2. ISCEV standard full-field ERGs (RE only) recorded from 2 patients diagnosed with ACHM (rows I – II) plus a data set from a representative of our normal control group (row III). Column 1: light adapted single flash response (3.0 cd/s/m^2); Column 2: 30Hz flicker stimulus (3.0 cd/s/m^2); Column 3; dark-adapted (rod only) response (0.01cd/s/m^2); Column 4: bright flash (10.0 cd/s/m^2).

*Figure 3. Dark-adapted ERGs generated by a series of stimuli of increasing retinal illuminance (-1.9 – 3.6 log scot trolands). ERGs from the age-matched normal control are shown in the first colu*mn with responses from the two *ACHM patients shown in columns 2-3. ERG responses were not recorded to the two highest luminances for Px 1.*

Figure 4. Plots of b-wave amplitude (A) and implicit time (B) and a-wave amplitude (C) and implicit time (D) as a function of retinal illuminance for the data shown in figure 3 for the 2 rod monochromats and the age-matched control subject.

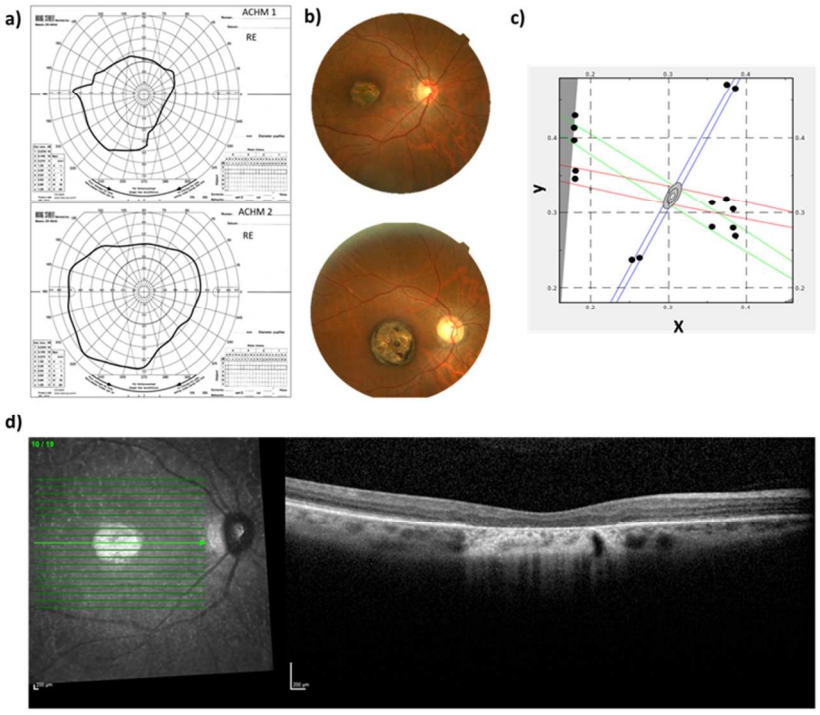

Figure 1. a) Goldman visual field plots, and b) fundus photographs for RE only of ACHM patients 1 & 2. c) Colour discrimination thresholds plotted on a CIE 1931 (xy) chromaticity diagram for 16 different coloured targets along red, green, blue & yellow colour axes. Normal colour discrimination thresholds (+/- 1 SD) are indicated by the central grey ellipse. Both rod monochromats (only data from Patient 2 are shown) exhibit elevated discrimination thresholds consistent with severe L-, M- and S-cone dysfunction. d) OCT image of macular region of the RE of ACHM patient 1.

81x60mm (300 x 300 DPI)

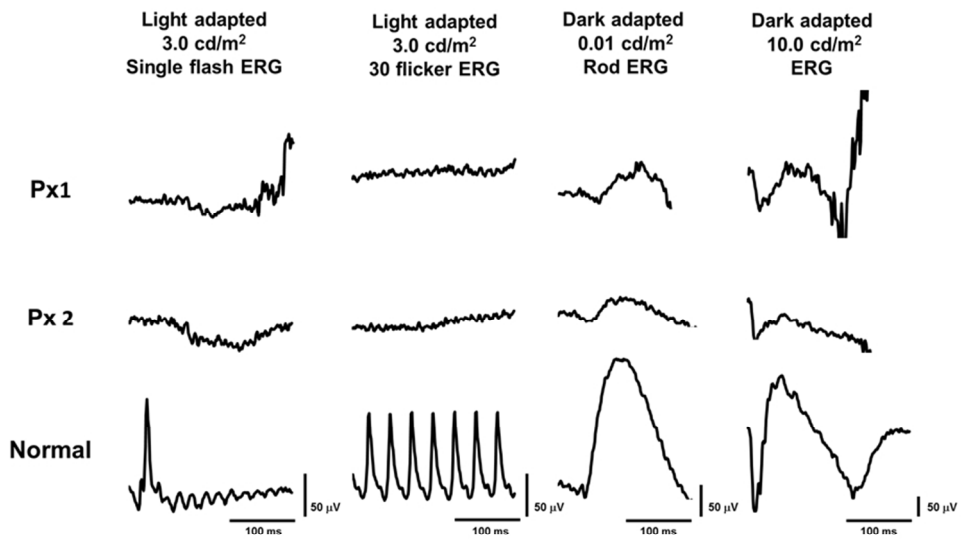

Figure 2. ISCEV standard full-field ERGs (RE only) recorded from 2 patients diagnosed with ACHM (rows I – II) plus a data set from a representative of our normal control group (row III). Column 1: light adapted single flash response (3.0 cd/s/m2); Column 2: 30Hz flicker stimulus (3.0 cd/s/m2); Column 3; dark-adapted (rod only) response (0.01cd/s/m2); Column 4: bright flash (10.0 cd/s/m2).

81x60mm (300 x 300 DPI)

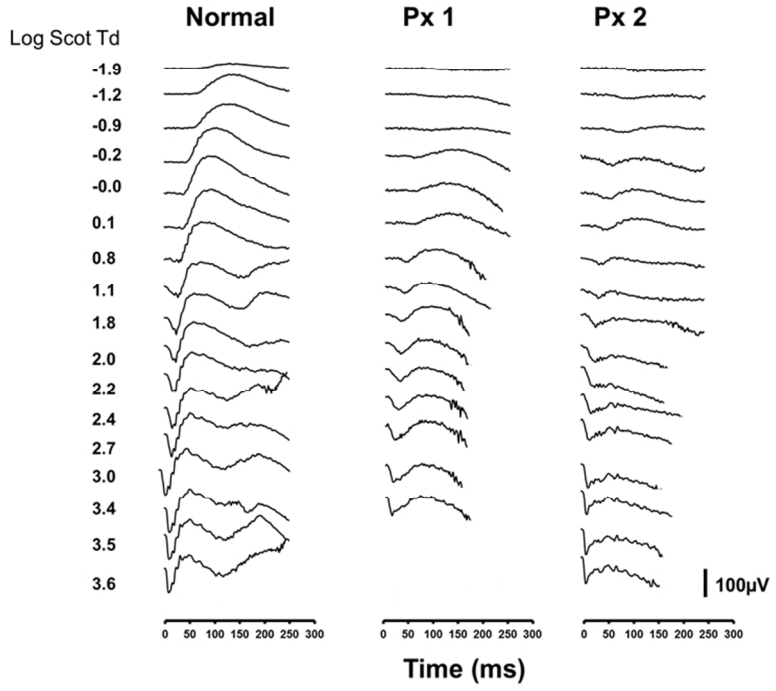

Figure 3. Dark-adapted ERGs generated by a series of stimuli of increasing retinal illuminance (-1.9 – 3.6 log scot trolands). ERGs from the age-matched normal control are shown in the first column with responses from the two ACHM patients shown in columns 2- 3. ERG responses were not recorded to the two highest luminances for Px 1.

81x60mm (300 x 300 DPI)

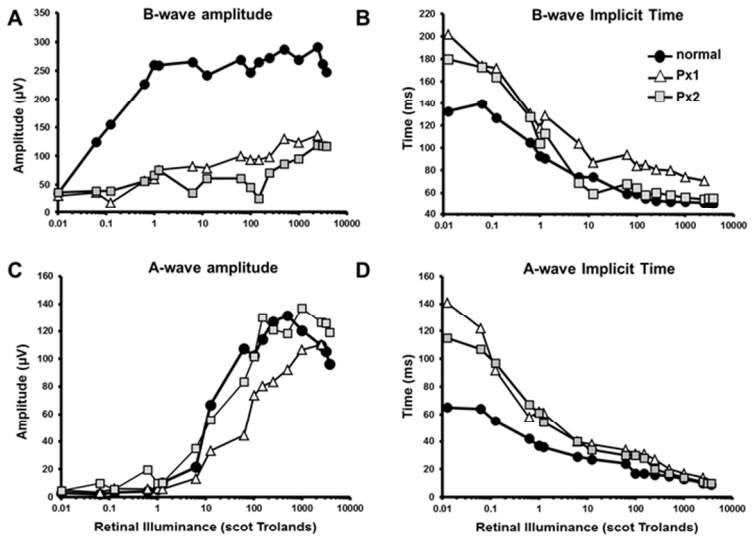

Figure 4. Plots of b-wave amplitude (A) and implicit time (B) and a-wave amplitude (C) and implicit time (D) as a function of retinal illuminance for the data shown in figure 3 for the 2 rod monochromats and the age-matched control subject.

81x60mm (300 x 300 DPI)